J|A|C|S ARTICLES

Published on Web 11/11/2010

Nitrotetrazolate-2*N*-oxides and the Strategy of *N*-Oxide Introduction

Michael Göbel,[†] Konstantin Karaghiosoff,[†] Thomas M. Klapötke,*[,†,‡] Davin G. Piercey,[†] and Jörg Stierstorfer[†]

Department of Chemistry and Biochemistry, Energetic Materials Research, Ludwig-Maximilian University of Munich, Butenandtstr. 5-13, D-81377 Munich, Germany, and Center for Energetic Concepts Development, CECD, University of Maryland, UMD, Department of Mechanical Engineering, College Park, Maryland 20742, United States

Received August 2, 2010; E-mail: tmk@cup.uni-muenchen.de

Abstract: The first anionic tetrazole-2*N*-oxide has been prepared by mild aqueous oxidation of easily prepared 5-nitrotetrazole with commercially available oxone in high yields. The result of protonating 5-nitrotetrazolate-2*N*-oxide has been identified as a hydroxytetrazole, and the nitrogen-rich salts including ammonium, hydroxylammonium, guanidinium, aminoguanidinum, diaminoguanidinium, and triaminoguanidinium have been prepared and characterized. When compared to the nitrogen-rich salts of nitrotetrazole, the nitrogen-rich salts of nitrotetrazole-2*N*-oxide show superior energetic performance as calculated by the EXPLO5 computer code, using heats of formation calculated using the CBS-4M level of quantum mechanical theory. The impact, friction, and electrical spark sensitivities of the nitrogen-rich nitrotetrazolate-2*N*-oxides were measured and cover the whole range from sensitive to insensitive energetic materials.

Introduction

The design of new energetic materials, encompassing all of propellants, explosives, and pyrotechnics, is a long-standing tradition in the chemical sciences. The chemistry of energetic materials has led to many advances in the chemical sciences, notably the concept of isomerism which was derived from the structural isomers silver fulminate and silver cyanate.[1] Due to the nature of energetic materials being on the borderline between existence and nonexistance, many historical chemists were drawn to this field including Liebig, Berzelius, and Gay-Lussac.[2,3] Energetic materials chemistry pushes the limits of the unique molecules that can be created, while retaining some semblance of stability. The design of modern energetic materials is a modern scientific challenge.[4−6] Currently used, outdated, energetics suffer from limitations that can be remedied by the tailoring at the molecular level of new energetic molecules. One of the most important characteristics of new energetic materials is that they can be characterized as "green" by not causing a toxicological problem or an environmental hazard. New energetics must also meet increased performance requirements, where propellants must transport ever-increasing payloads, explosives must become more powerful, and pyrotechnics demands a greater range and purity of spectral emissions.[7] Exemplifying these problems is the quintessential commonly used explosive, RDX (1,3,5-trinitro-1,3,5-triazinane), a potential carcinogen,[8] and possessing nitramines it is known to be toxic to vital organisms at the base of the food chain.[9] In particular, RDX is also sensitive to physical stimuli so for use it must be stabilized.[10] Technical challenges facing today's synthetic energetic chemists include the preparation of new energetic materials with performance equal to or surpassing that of RDX, while tailoring them for high personal and ecological safety.[11−13]

Traditional energetic materials such as TNT (2,4,6-trinitrotoluene) and RDX derive the majority of their energy from the oxidation of a carbon backbone and the presence of both fuel and oxidizer in the same molecule. New trends in the research and development of novel energetics have introduced two other classes of energetic materials: high heat of formation, nitrogen-rich materials (e.g., high-nitrogen heterocyclics such as tetrazoles, and tetrazines) and caged and cyclic compounds (e.g., cubane based energetics).[7] Naturally, these strategies can and have been combined making high-nitrogen, strained, heterocycles an intense area of research.

[†] Ludwig-Maximilian University of Munich.
[‡] University of Maryland.

(1) Gay-Lussac, J. L. *Ann. Chem. Phys.* **1824**, *27* (2), 199.
(2) Gay-Lussac, J. L.; Leibig, J. *Kastners Archiv* **1824**, *II*, 58–91.
(3) Berzelius, J. *Ann. Chem. Pharm.* **1844**, *L*, 426–429.
(4) Davis, T. L. *The Chemistry of Powder and Explosives*; Angriff, Los Angeles, 1943; pp 424−430.
(5) De Yong, L. V.; Campanela, J. J. *Hazard Mater.* **1989**, *21*, 125–133.
(6) Klapötke, T. M.; Sabaté, C. M. *Heteroatom. Chem.* **2008**, *19*, 301–305.
(7) Klapötke, T. M. *High Energy Density Materials*; Springer: 2007.
(8) McLellan, W.; Hartley, W. R.; Brower, M. *Health advisory for hexahydro-1,3,5-trinitro-1,3,5-triazine*. Technical report PB90−273533; Office of Drinking Water, U.S. Environmental Protection Agency: Washington, DC, 1988.
(9) Robidoux, P. Y.; Hawari, J.; Bardai, G.; Paquet, L.; Ampleman, G.; Thiboutot, S.; Sunahara, G. I. *Arch. Environ. Contam. Toxicol.* **2002**, *43*, 379–388.
(10) Bowers, R. C.; Romans, J. B.; Zisman, W. A. *Ind. Eng. Chem. Prod. Res. Dev.* **1973**, *12* (1), 2–13.
(11) Altenburg, T.; Klapötke, T. M.; Penger, A.; Stierstorfer, J. *Z. Anorg. Allg. Chem.* **2010**, *636*, 463–471.
(12) Klapötke, T. M.; Sabaté, C. M. *Z. Anorg. Allg. Chem.* **2009**, *635*, 1812–1822.
(13) Fischer, N.; Karagiosoff, K.; Klapötke, T. M.; Stierstorfer, J. *Z. Anorg. Allg. Chem.* **2010**, *636*, 735–739.

 10.1021/ja106892a

For a nitrogen-rich, endothermic material, possessing ring or cage strain, to find application as a high explosive it needs to possess high thermal and mechanical stabilities, while at the same time satisfying the increasing demand for higher performing materials. Unfortunately, in many cases high performance and low sensitivity appear to be mutually exclusive; many high performing materials are not stable enough to find practical use, and many materials with the desired sensitivity do not possess the performance requirements of a material to replace a commonly used explosive.[14] This trend is exemplified in the range of five-membered azoles from pyrazole to pentazole, where pyrazole is not used in energetics due to low performance, and the few pentazole derivatives known are highly unstable.[15] One of the most promising heterocyclic backbones for the preparation of high-performing energetics is the tetrazole ring.

Possessing high heats of formation resulting from the nitrogen−nitrogen bonds, ring strain, and high density, the tetrazole ring has allowed the preparation of high-performing primary[16] and secondary[17] explosives. Depending on the ring substitutents and anion/cation pairing, tetrazole based energetics can be tailored to span the spectrum of sensitivity from insensitive to highly sensitive (primary explosives). The sensitivity of 5-substituted anionic tetrazole based explosive materials decreases in the order of $N_2^+ > N_3 > NO_2 > Cl > NNO_2 > H > NH_2 > CH_3$ as a function of the electron-withdrawing nature of the substituent.[18] Additionally, due to their aromatic ring, tetrazoles are generally thermally stable.[19]

Other than the high heats of formation, for a molecule or salt to be a high-performing energetic, a high oxygen balance is required. The oxygen balance is a percentage representation of the oxygen content of a compound, enabling it to oxidize all of its nonoxidizing content to their respective oxides and is easily calculated by the equation $\Omega\ (\%) = (w\mathrm{O} - 2x\mathrm{C} - 1/2y\mathrm{H} - 2z\mathrm{S}) \cdot 1600/M$ (w: number of oxygen atoms, x: number of carbon atoms, y: number of hydrogen atoms, z: number of sulfur atoms). A current limitation of current tetrazole-based energetic materials is the low oxygen balances.[13,20,21] Anionic tetrazole oxygen balances are limited by the explosophore of choice on position 5 of the ring, the carbon atom. High-performance tetrazole-based energetics often contain nitro,[21] nitrimino,[13] or azido[20] functionalities upon the carbon of position 5, and at most these contain two oxygen atoms, only sufficient for the oxidation of the tetrazole carbon to carbon dioxide, however, not enough to oxidize any nitrogen-rich, oxygen-lacking energetic cation (e.g., aminoguanidinium, diaminoguanidinium) paired with the energetic tetrazole. There is a pressing need in the energetic materials field to be able to incorporate more oxygen atoms onto derivatives of the already high-performing tetrazole ring. Introducing *N*-oxides onto the tetrazole ring may prove to be a viable solution to this challenge and may push the limits of well-explored tetrazole chemistry into a new, unexplored, dimension.

Amine *N*-oxides are a strategy of increasing density, stability, and performance of energetic materials and has found use in insensitive explosives.[22] Their zwitterionic structure and large dipole moment allow for the formation of compounds with high densities,[23] while simultaneously increasing their oxygen balance compared to the nonoxide amine. For example, comparison of 2,4,6-trinitropyridine to 2,4,6-trinitropyridine-1-oxide shows both a higher density and as such higher energetic performance.[24] The stabilizing effects of the *N*-oxide on a nitrogen-rich system is well-known; for example, 1,2,3,4-tetrazines are uncommon in the literature with only a single compound claimed to exist.[25] In contrast, the 1,2,3,4-tetrazine-1,3-dioxides are well-known and show remarkably high stabilities, with many members of this highly energetic class of compounds decomposing above 200 °C.[25] For high-nitrogen systems, the source of this stabilization has been calculated to be resultant from the *N*-oxide removing lone pair electron density (increasing $\sigma-\pi$ separation) that would otherwise destabilize the nitrogen system by donating electron density into antibonding orbitals.[26−28]

Tetrazole oxides are uncommon in the literature. The tetrazole 1*N*-oxides are only slightly more common than the 2*N*-oxides with a handful of compounds and preparations known in the literature; the first 2*N*-oxides were only described in 2010. The 1*N*-oxides have been prepared by the rearrangement of 1-alkoxy tetrazoles either by high temperature[29] or by means of trifluoroacetic acid.[30] Also known is the reaction of toxic HN_3 with nitrolic acids to produce tetrazole 1*N*-oxides.[31] The tetrazole 2*N*-oxides were not known until earlier this year, where 1,5-disubstituted tetrazoles were successfully oxidized with hypofluorous acid in acetonitrile to give 1,5-disubstituted tetrazole-2*N*-oxides.[32] This was the first preparation of a tetrazole oxide by oxidation of the tetrazole ring, widely thought impossible prior as a result of the low HOMO in tetrazoles,[33] where previous attempts at forming oxides on the tetrazole ring only led to hydroxy compounds.[34,35] To date, anionic tetrazole 2*N*-oxides are unknown in scientific literature.

We have developed a procedure for the mild, aqueous, oxidation of nitrotetrazole to the corresponding nitrotetrazolate-2*N*-oxide. The base nitrotetrazole anion was first synthesized

(14) Sikder, A. K.; Sikder, N. *J. Hazard. Mater.* **2004**, *112*, 1–15.
(15) Carlqvist, P.; Östmark, H.; Brinck, T. *J. Phys. Chem. A* **2004**, *108*, 7463–7467.
(16) Huynh, M. H. V.; Hiskey, M. A.; Meyer, T. J.; Wetzler, M. *Proc. Natl. Acad. Sci. U.S.A.* **2006**, *103* (14), 5409–5412.
(17) Boese, R.; Klapötke, T. M.; Mayer, P.; Verma, V. *Propellants, Explos., Pyrotech.* **2006**, *31* (4), 263–268.
(18) Zhao-Xu, C.; Heming, X. *Int. J. Quantum Chem.* **2000**, *79*, 350–357.
(19) Stierstorfer, J.; Klapötke, T. M.; Hammerl, A.; Chapman, R. D. *Z. Anorg. Allg. Chem.* **2008**, *634*, 1051–1057.
(20) Klapötke, T. M.; Stierstorfer, J. *J. Am. Chem. Soc.* **2009**, *131*, 1122–1134.
(21) Klapötke, T. M.; Mayer, P.; Sabaté, C. M.; Welch, J. M.; Wiegand, N. *Inorg. Chem.* **2008**, *47* (13), 6014–6027.
(22) Zhang, C.; Wang, X.; Huang, H. *J. Am. Chem. Soc.* **2008**, *130* (26), 8359–8365.
(23) Molchanova, M. S.; Pivina, T. S.; Arnautova, E. A.; Zefirov, N. S. *J. Mol. Struct.* **1999**, *465*, 11–24.
(24) Jia-Rong, L.; Jian-Min, Z.; Hai-Shan, D. *J. Chem. Crystallogr.* **2005**, *35* (12), 943–948.
(25) Churakov, A. M.; Tartakovsky, V. A. *Chem. Rev.* **2004**, *104*, 2601–2616.
(26) Glukhovtsev, M. N.; Simkin, B. Y.; Minkin, V. I. *Zh. Organicheskoi Khim.* **1988**, *24* (12), 2486–2488.
(27) Inagake, S.; Goto, N. *J. Am. Chem. Soc.* **1987**, *109*, 3234–3240.
(28) Noyman, M.; Zilberg, S.; Haas, Y. *J. Phys. Chem. A* **2009**, *113*, 7376–7382.
(29) Plenkiewicz, J.; Roszkiewicz, A. *Pol. J. Chem.* **1993**, *67* (10), 1767–1778.
(30) Liepa, A. J.; Jones, D. A.; McCarthy, T. D.; Nearn, R. H. *Aust. J. Chem.* **2000**, *53* (7), 619–622.
(31) Maffei, S.; Bettinetti, G. F. *Ann. Chim. (Rome, Italy)* **1956**, *46*, 812–815.
(32) Harel, T.; Rozen, S. *J. Org. Chem.* **2010**, *75*, 3141–3143.
(33) Eicher, T.; Hauptman, S. *The Chemistry of Heterocycles*, 2nd ed.; Wiley: 2003; p 212.
(34) Begtrup, M.; Vedsoe, P. *J. Chem. Soc., Perkin Trans. 1* **1995**, 243–247.
(35) Giles, R. G.; Lewis, N. J.; Oxley, P. X.; Quick, J. K. *Tetrahedron Lett.* **1999**, *40*, 6093–6094.

Scheme 1. Oxidation of Nitrotetrazolate to the Nitrotetrazolate-2*N*-oxide Anion

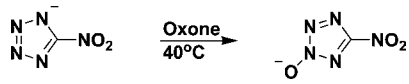

over 75 years ago by von Herz and has enjoyed the ability to form next-generation "green" primary explosives.[16] Additionally, the nitrogen-rich salts[21] and covalent compounds[17] of nitrotetrazole are potential green replacements of currently used secondary explosives. Possessing a wide spectrum of fully characterized compounds with various properties, nitrotetrazole proved to be an ideal candidate for oxidation to the nitrotetrazole-2*N*-oxide allowing comparison of the properties of our newly prepared nitrogen-rich nitrotetrazolate-2*N*-oxides with the corresponding nitrotetrazolates.

Beyond application as energetic materials, tetrazole oxides may find application for medicinal purposes as both *N*-oxides[36,37] and tetrazoles have known biological activity.[38]

Herein we report on the synthesis and characterization of a series of highly energetic nitrogen- and oxygen-rich salts containing the nitrotetrazolate 2*N*-oxide anion. The compounds prepared were characterized by X-ray diffraction, infrared and Raman spectroscopy, multinuclear NMR spectroscopy, elemental analysis, and DSC. Computational calculations predicting energetic performance properties confirm the initial hypothesis that oxidation of tetrazoles to tetrazole oxides is indeed an effective method of improving energetic performance. We expand the field of tetrazole chemistry by offering the first synthesis of an anionic tetrazole 2*N*-oxide in a high-yielding, aqueous synthesis starting from the parent tetrazole. We have exemplarily demonstrated the ability of this new class of compounds to form high performance, energetic materials based on nitrogen-rich salts of the nitrotetrazole-2*N*-oxide moiety.

Results and Discussion

Synthesis. The most facile synthesis of the nitrotetrazolate-2*N*-oxide anion is by the oxidation of ammonium 5-nitrotetrazolate hemihydrate in a saturated oxone solution at 40 °C (Scheme 1).

The free acid **2** and salts **3**−**6** were prepared from the ammonium salt by simple acid−base chemistry and metathesis reactions with either acid or (amino) guanidinium (bi) carbonate, while salts **7** and **8** were prepared from the silver salt **6** and the corresponding substituted guanidinium halide (Scheme 2). Salt **3** was prepared by ion exchange.

CAUTION. *5-Nitrotetrazole-2N-oxide (**2**) and its salts (**1**, **3**−**8**) are all energetic compounds with sensitivity to various stimuli. While we encountered no issues in the handling of these materials, proper protective measures (face shield, ear protection, body armor, Kevlar gloves, and earthened equipment) should be used at all times.*

The oxidation of ammonium nitrotetrazolate hemihydrate in a saturated aqueous Oxone solution proceeds smoothly at 40 °C over three days. Acidification of the reaction liquors allowed separation of the crude protonated nitrotetrazolate-2*N*-oxide,

Scheme 2. Prepared Salts of Nitrotetrazolate-2*N*-oxide

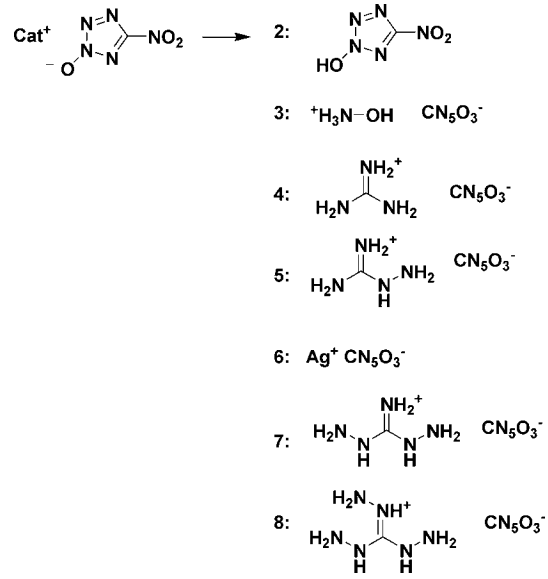

which after reaction with dilute, aqueous ammonia yielded ammonium nitrotetrazolate-2*N*-oxide. The ammonium salt (ANTX, **1**) was purified by recrystallization from acetonitrile yielding crystals suitable for X-ray diffraction. The free acid 5-nitrotetrazole-2*N*-oxide (**2**) was extracted from an acidic solution of the aqueous ammonium salt with ether; it is extremely deliquescent, dissolving itself in absorbed water after only a few minutes of exposure to air. Crystals of **2** were grown by slow evaporation of an ether/toluene solution under vacuum. The hydroxylammonium salt (HxNTX, **3**) was prepared by ion-exchanging the ammonium salt and recrystallizing from acetonitrile. The crystals grown this way contained a molecule of acetonitrile which was lost upon drying under high vacuum; crystals suitable for X-ray diffraction were grown from slow evaporation of an ethyl acetate solution. Guanidinium (GNTX, **4**) and aminoguanidinium (AGNTX, **5**) salts were prepared by refluxing an ethanolic solution of **1** with the corresponding carbonate or bicarbonate. After 24 h the aminoguanidinium salt was isolated as crystals suitable for X-ray diffraction upon cooling; however, the guanidinium salt required ether diffusion into a methanolic solution in order to obtain crystals. Preparation of diaminoguanidinium (DAGNTX, **7**) and triaminoguanidinium (TAGNTX, **8**) nitrotetrazolate-2*N*-oxide required the preparation of silver nitrotetrazolate-2*N*-oxide from the ammonium salt and aqueous silver nitrate in stoichiometric quantities. The silver salt (**6**) precipitates as a flocculent precipitate slightly soluble in water. The silver salt (**6**) is not a sensitive primary explosive unlike silver nitrotetrazolate[21] and can be safely handled. **6** was easily reacted with aqueous diaminoguanidinium iodide or triaminoguanidinium chloride, which after filtration of the precipitated silver halide, and evaporation of water, yielded pure diaminoguanidinium nitrotetrazolate-2*N*-oxide (**7**) and triaminoguanidinium nitrotetrazolate-2*N*-oxide (TAGNTX, **8**), after recrystallization from ethanol. Crystals suitable for X-ray diffraction were grown for both **7** and **8** by the slow diffusion of ether into a methanolic solution of the material.

Spectroscopy. Multinuclear NMR spectroscopy, especially ^{13}C and ^{15}N spectroscopy, proved to be a valuable tool for the characterization of the tetrazole and tetrazolates. With the exception of the free acid **2**, all NMR spectra were performed in DMSO-d_6. The extreme acidity of **2** mandated NMR

(36) Pyatakova, N. V.; Khropov, Y. V.; Churakov, A. M.; Tarasova, N. I.; Serezhenkov, V. A.; Vanin, A. F.; Tartakovsky, V. A.; Severina, I. S. *Biokhimiya* **2002**, *67* (3), 396–402.
(37) Boiani, M.; Cerecetto, H.; Gonzáles, M.; Risso, M.; Olea-Azar, C.; Piro, O. E.; Castellano, E. E.; Ceráin, A. L.; Ezpeleta, O.; Monge-Vega, A. *Eur. J. Med. Chem.* **2001**, *36*, 771–782.
(38) Jin, T.; Kamijo, S.; Yamamoto, Y. *Tetrahedron Lett.* **2004**, *45*, 9435–9437.

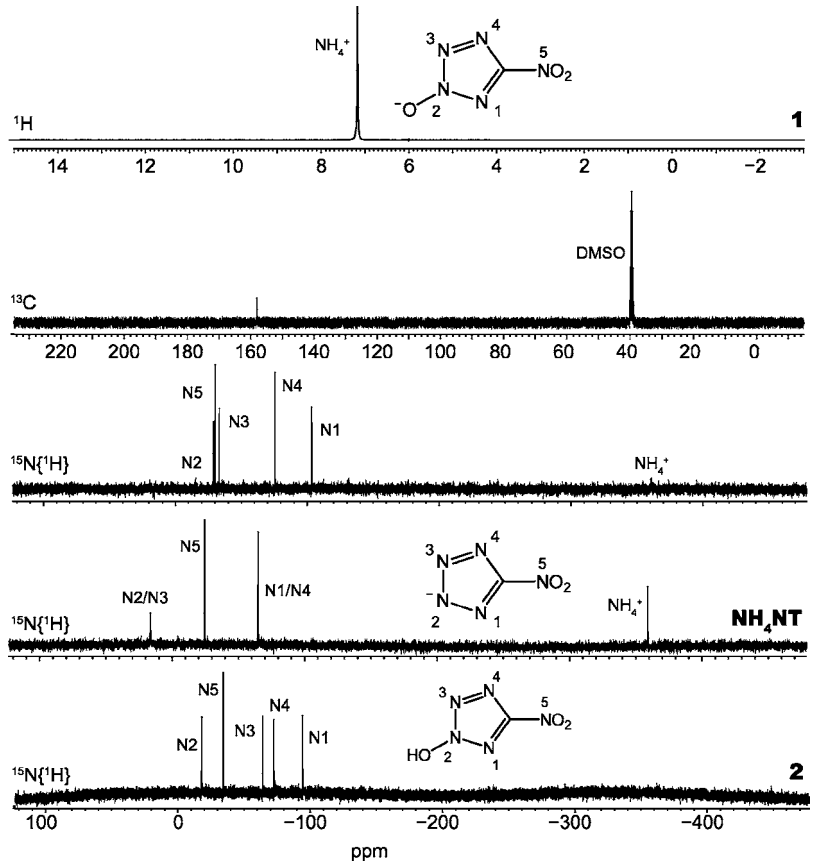

Figure 1. Multinuclear (^{1}H, ^{13}C, and ^{15}N) spectra of ANTX (**1**) compared to ^{15}N spectra of ammonium nitrotetrazolate (NH_4NT) and free acid (**2**).

experiments to be performed in THF-d_8; spectra could not be measured in DMSO-d_6 as **2** is a strong acid, protonating DMSO, and attempts to perform NMR in acetone-d_6 led to polymerization of the acetone. In all anionic nitrotetrazolate-2*N*-oxides the single ^{13}C carbon shift for the $CN_5O_3^-$ anion lies near 158 ppm. In the free acid (**2**) the ^{13}C shift for CN_5O_3H shifts downfield to 162 ppm. Figure 1 illustrates the ^{1}H, ^{13}C, and ^{15}N NMR spectra of ANTX (**1**). The ammonium protons occur as a broad singlet at ∼7.4 ppm, similar to that in ammonium nitrotetrazolate,[21] and the ^{13}C shift of 158.4 ppm is approximately 10 ppm upfield compared with the ^{13}C shift of 169.5 ppm in ammonium nitrotetrazolate.[21] When the ^{15}N spectrum of ANTX (**1**) is compared with that of ammonium nitrotetrazolate (Figure 1), a loss of nitrogen equivalency is seen between N1 and N4 and between N2 and N3. The largest change in chemical shift for a ring nitrogen between the nitrotetrazolate ion and the nitrotetrazolate-2*N*-oxide ion is for N2, where in nitrotetrazolate N2's chemical shift occurs at 16.4 ppm, but in nitrotetrazolate-2*N*-oxide this peak has shifted to −33.3 ppm. The remainder of the peak assignments were made after the determination that the largest peak shift would belong to the nitrogen onto which the *N*-oxide has been added (Figure 1). Protonation of the nitrotetrazolate-2*N*-oxide anion yields highly acidic **2**, with a proton resonance at 12.99 ppm. This is out of the range for an acidic N−H proton, as even 5-nitrotetrazole with a pK_a of −0.8[39] has its proton shift at 6.29 ppm.[40] This high ^{1}H shift along with the ^{15}N NMR (Figure 1), where the largest N shift compared to that of the nitrotetrazolate-2*N*-oxide anion is for N2 led to the determination that the nitrotetrazolate-2*N*-oxide protonates forming a 2-hydroxy-5-nitrotetrazole. Lack of N−H coupling in the ^{15}N spectrum supports this conclusion. ^{15}N signal assignments (Figure 1) were made based on comparison with our ^{15}N spectra of nitrotetrazolate-2*N*-oxide and with the ^{15}N spectrum of 5-nitrotetrazole.[40]

The IR and Raman spectra of all compounds were recorded and assigned using frequency analysis from an optimized structure (B3LYP/cc-pVDZ using the Gaussian 03 software).[41] All calculations were performed at the DFT level of theory; the gradient-corrected hybrid three-parameter B3LYP[42,43] functional theory has been used with a correlation consistent cc-pVDZ basis set.[44−47] The anionic nitrotetrazole-2*N*-oxides generally contain a strong, diagnostic band in the infrared ranging from 1531 to 1551 cm^{-1}. The calculated value for this band is 1549 cm^{-1}, and it arises from the N−O stretch, with a minor constitution of asymmetric NO_2 stretching and the N1−N2−N3 symmetric tetrazole ring in phase deformation. The Raman spectra of all salts of nitrotetrazolate-2*N*-oxide all adopt

(39) Koldobskii, G. I.; Soldatenko, D. S.; Gerasimova, E. S.; Khokryakova, N. R.; Shcherbinin, M. B.; Lebedev, V. P.; Ostrovskii, V. A. *Russ. J. Org. Chem.* **1997**, *33* (12), 1771–1783.
(40) Klapötke, T. M.; Sabaté, C. M.; Stierstorfer, J. *New J. Chem.* **2009**, *33*, 136–147.
(41) Frisch, M. J. *Gaussian 03*, revision C.03: see ref 1 in the Supporting Information
(42) Becke, A. D. *J. Chem. Phys.* **1993**, *98*, 5648–5652.
(43) Lee, C.; Yang, W.; Parr, R. G. *Phys. Rev. B* **1988**, *37*, 785–789.
(44) Woon, D. E.; Dunning, T. H., Jr. *J. Chem. Phys.* **1993**, *98*, 1358–1371.
(45) Kendall, R. A.; Dunning, T. H., Jr.; Harrison, R. J. *J. Chem. Phys.* **1992**, *96*, 6796–6806.
(46) Dunning, T. H., Jr. *J. Chem. Phys.* **1989**, *90*, 1007–1023.
(47) Peterson, K. A.; Woon, D. E.; Dunning, T. H., Jr. *J. Chem. Phys.* **1994**, *100*, 7410–7415.

Table 1. Relative Energies of Protonation Sites on the Nitrotetrazolate-2*N*-oxide Anion

	N1−H	N3−H	N4−H	O−H
Point group	*Cs*	*Cs*	*Cs*	*Cs*
$-E$ (a.u.)	537.930 995	537.936 350	537.935 818	537.943 076
El. state	$^1A'$	$^1A'$	$^1A'$	$^1A'$
NIMAG	0	0	0	0
zpe (kcal/mol)	33.1	33.5	33.5	33.3
E_{rel} (kcal/mol)	7.6	4.2	4.6	0.0

a diagnostic pattern of three bands of high intensity. The first of these occurs in the range of 1407−1421 cm^{-1} (calcd 1431 cm^{-1}) and corresponds to a combined C−NO_2 stretch and an asymmetric C1−N4−N3 in a phase tetrazole ring stretch. The next of these occurs at 1048−1112 cm^{-1} (calcd 1060 cm^{-1}) and corresponds to N1−N2 stretching, in-phase tetrazole ring deformation, and C−NO_2 stretching. The final diagnostic stretch at 984−1010 cm^{-1} (calcd 918 cm^{-1}) corresponds to N2−N3 stretching with a small component of NO_2 asymmetric stretching. Due to its deliquescent nature, the acid (**2**), Raman proved to be a far more effective method of characterization compared to IR, as the water present resulted in broad bands in the IR, whereas in the Raman bands were sharp. The intense peak at 1423 (1433 calcd) cm^{-1} is a combination of a symmetric NO_2 stretch and an asymmetric, in-phase, N1−C5−N4 stretch. The next most intense Raman band at 1037 (1040 calcd) cm^{-1} is an in-plane asymmetric stretch of the tetrazole ring. The N−O stretch of the tetrazole oxide occurs at 761 (751 calcd) cm^{-1} with a significant component of this motion being the symmetric N1−N2−N3 deformation of the tetrazole ring. At 412 (402 calcd) cm^{-1} is the in-plane rocking of the N−O and the C−NO_2. These assignments supported the assignment of compound **2**, resulting from the protonation of nitrotetrazolate-2*N*-oxide, as being a hydroxytetrazole as opposed to being a ring-protonated species.

Table 2. Crystallographic Data and Structure Refinement Details for Compounds **1**−**5** and **7**−**8**

compound	ANTX (**1**)	HNTX (**2**)	HxNTX (**3**)	GNTX (**4**)	AGNTX (**5**)	DAGNTX (**7**)	TAGNTX (**8**)
formula	$C_1H_4N_6O_3$	$C_1H_1N_5O_3$	$C_1H_4N_6O_4$	$C_2H_6N_8O_3$	$C_2H_7N_9O_3$	$C_2H_8N_{10}O_3$	$C_2H_9N_{11}O_3$
formula weight [g mol^{-1}]	148.10	131.07	164.10	190.15	205.17	220.18	235.20
temperature [K]	100	173	173	173	173	173	173
crystal system	orthorhombic	monoclinic	monoclinic	triclinic	monoclinic	triclinic	monoclinic
space group	*Pbca*	*Cc*	$P2_1/c$	$P\bar{1}$	$P2_1/c$	$P\bar{1}$	$P2_1/c$
a [Å]	9.3989(4)	7.9946(6)	8.489(5)	6.0610(8)	7.812(3)	6.4344(6)	10.267(3)
b [Å]	7.9263(3)	9.1402(6)	12.341(5)	7.5528(9)	15.783(2)	8.0055(7)	12.622(2)
c [Å]	15.2618(6)	6.2269(4)	5.626(5)	8.2886(9)	6.619(3)	8.5160(8)	7.370(3)
α [deg]	90	90	90	79.360(10)	90	90.218(7)	90
β [deg]	90	99.584(6)	91.221(5)	89.576(10)	100.194(5)	94.461(7)	93.724(5)
γ [deg]	90	90	90	85.918(11)	90	97.519(7)	90
volume [$Å^3$]	1136.98(8)	448.66(5)	589.3(7)	371.96(8)	803.2(5)	433.53(7)	953.1(5)
formula *Z*	8	4	4	2	4	2	4
space group *Z*	8	4	4	2	4	2	4
density calcd [g cm^{-3}]	1.7304(1)	1.9404(2)	1.850(2)	1.6978(4)	1.6967(17)	1.6867(3)	1.6391(15)
R_1/wR_2 [all data]	0.0336/0.0659	0.0270/0.0437	0.0349/0.0592	0.1166/0.2089	0.0795/0.0582	0.0800/0.0887	0.0607/0.0753
R_1/wR_2 [$I > 2\sigma(I)$]	0.0259/0.0638	0.0220/0.0428	0.0246/0.0571	0.0760/0.1943	0.0359/0.0538	0.0383/0.0799	0.0332/0.0699
S	0.958	0.921	0.928	0.906	0.842	0.861	0.99
CCDC	783 533	783 532	783 534	783 535	783 536	783 537	783 538

Table 3. Comparison of Selected Bond Lengths and Angles of Compounds **1**−**5** and **7**−**8** to the Corresponding 5-Nitro-2*H*-tetrazol Derivatives[a]

	Bond lengths/Å					Bond angles (deg)						
	N1−N2	N2−N3	N3−N4	N4−C1	C1−N1	C1−N1−N2	N1−N2−N3	N2−N3−N4	N3−N4−C1	N4−C1−N1	N2−O1	ρ/Δ
1 ANTX	1.33	1.34	1.34	1.32	1.33	99.4	114.9	105.2	105.0	115.6	1.301	1.730/+0.09
3 HxNTX	1.32	1.33	1.34	1.32	1.33	99.1	115.4	105.2	104.3	116.0	1.306	1.850/+0.13
4 GNTX	1.34	1.34	1.35	1.32	1.33	99.3	114.3	105.5	104.3	116.7	1.286	1.698/+0.05
5 AGNTX	1.33	1.34	1.35	1.32	1.33	99.7	114.1	105.6	104.5	116.1	1.288	1.697/+0.04
7 DAGNTX	1.32	1.34	1.35	1.32	1.34	99.4	114.9	105.9	105.2	114.5	1.273	1.687/+0.09
8 TAGNTX	1.33	1.33	1.34	1.32	1.34	99.3	114.3	106.0	104.3	116.1	1.293	1.639/+0.04
Average	1.33	1.34	1.34	1.32	1.33	99.4	114.6	105.5	104.5	116.1	1.295	1.717/+0.07
10 ANT[21]	1.33	1.33	1.34	1.32	1.32	103.7	109.3	109.7	103.2	114.1	−	1.637/−0.09
11 HyNT[21]	1.34	1.32	1.34	1.32	1.32	103.0	109.5	109.9	102.8	114.8	−	1.72/−0.13
12 GNT[21]	1.34	1.33	1.34	1.33	1.34	102.5	110.0	110.0	102.5	115.2	−	1.644/−0.05
13 AGNT[21]	1.34	1.32	1.34	1.31	1.32	102.8	109.7	109.7	103.1	114.8	−	1.661/−0.04
14 DAGNT[21]	1.34	1.32	1.34	1.31	1.31	102.9	109.6	109.5	102.8	115.3	−	1.595/−0.09
15 TAGNT[21]	1.35	1.34	1.35	1.33	1.33	102.9	109.7	109.3	103.1	114.9	−	1.601/−0.04
Average	1.34	1.33	1.34	1.32	1.32	103.0	109.6	109.7	102.9	114.9	−	1.643/−0.07
2 HNTX	1.31	1.32	1.32	1.34	1.32	98.9	115.5	104.5	105.0	115.1	1.344	1.940/+0.04
9 HNT[40]	1.32	1.32	1.32	1.34	1.31	98.9	115.5	105.5	104.2	115.9	−	1.899/−0.04

[a] HNT = 5-nitro-2*H*-tetrazol; ANT = ammonium 5-nitro-2*H*-tetrazolate; HyNT = hydrazinium 5-nitro-2*H*-tetrazolate; GNT = guanidinium 5-nitro-2*H*-tetrazolate, AGNT = aminoguanidinium 5-nitro-2*H*-tetrazolate; DAGNT = diaminoguanidinium 5-nitro-2*H*-tetrazolate; TAGNT = triaminoguanidinium 5-nitro-2*H*-tetrazolate; ρ = calculated crystal density/g cm^{-3}, Δ = difference to corresponding structure containing/missing the *N*-oxide moiety.

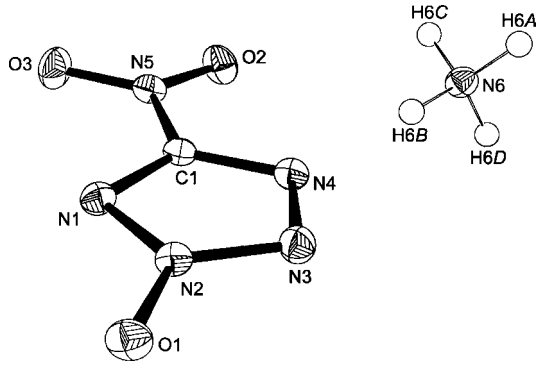

Figure 2. ORTEP representation of the molecular structure of **1** (ANTX, ammonium 5-nitrotetrazolate-2*N*-oxide) in the crystalline state. Displacement ellipsoids are shown at the 50% probability level.

Relative Energy. To support the NMR data in that the nitrotetrazolate-2*N*-oxide anion is protonated on the oxygen forming 2-hydroxy-5-nitrotetrazole, the relative energies of N1−H, N3−H, and N4−H ring-protonated species were calculated. The calculations performed were in accordance with the same software, theory, and basis set as described in the vibrational spectroscopy section. The relative energies calculated indicate that the 2-hydroxy-5-nitrotetrazole is the lowest energy species formed from the protonation of the nitrotetrazolate-2*N*-oxide anion (Table 1).

Single Crystal X-ray Structure Analysis. Compounds **1**−**5** as well as **7**−**8** have been characterized using single crystal X-ray structure determination. Table 2 summarizes a selection of crystallographic data and refinement details. A comparison of selected bond length and angles of compounds **1**−**5** and **7**−**8** and to the corresponding compounds **9**−**15** bearing no *N*-oxide moiety is given in Table 3. The data reveal that bond length values of both groups of anions are comparable within the limits of error in contrast to their bond angles. The average $N_1-N_2-N_3$ bond angle of the *N*-oxide anions has a value of 114.6° as compared to an average value of 109.6° of the *N*-oxide free nitrotetrazolate anions (Table 3) indicative of the higher sp^2 type hybridization of the *N*-oxide nitrogen atom. In contrast, the two neighboring angles ($C_1-N_1-N_2$ *N*-oxide: 99.4°/parent compound: 103.0°, $N_2-N_3-N_4$ *N*-oxide: 105.5°/parent compound: 109.7°) have smaller values yielding a slightly distorted tetrazole moiety in the 5-nitrotetrazolate-2*N*-oxide anions compared to the symmetric structure of the tetrazole in the parent nitrotetrazolate anions. This difference is not observed in the case of the corresponding free acids. Both 5-nitro-2*H*-tetrazole (**9**, HNT) and 2-hydroxy-5-nitrotetrazole (**2**, HNTX) share comparable bond lengths and angles (cf. Table 3). The most striking difference between the *N*-oxide containing compounds and their parent relatives is observed in their extended structures. Each of the compounds **1**−**5** and **7**−**8** has a higher crystal density compared to the corresponding *N*-oxide free compound as a consequence of the *N*-oxide being involved in multiple intermolecular bonding interactions as exemplified in the case of **1** and **2** (cf. Figures 3 and 5).

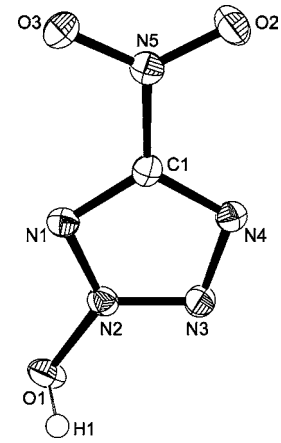

Figure 4. ORTEP representation of the molecular structure of **2** (2-hydroxy-5-nitrotetrazole, HNTX) in the crystalline state. Displacement ellipsoids are shown at the 50% probability level.

The structure of **1** (ANTX, ammonium 5-nitrotetrazolate-2*N*-oxide) at 100 K has orthorhombic (*Pbca*) symmetry. The asymmetric unit consists of one molecule (Figure 2).

The extended structure of **1** consists of two-dimensional ribbons of 5-nitrotetrazolate-2*N*-oxide anions interconnected via hydrogen bonding ($N-H\cdots O_{N\text{-oxide}}$, $N-H\cdots O_{\text{nitro group}}$, $N-H\cdots N_{\text{ring}}$) through each of the hydrogen atoms of the ammonium cations. Additionally, one of the oxygen atoms of the nitro group is involved in an interaction with the π electrons of the tetrazole ring (Figure 3).

The structure of **2** (2-hydroxy-5-nitrotetrazole, HNTX) at 173 K has monoclinic (*Cc*) symmetry. The asymmetric unit consists of one molecule (Figure 4).

The remarkably high density of 1.9404(2) g cm^{-3} can be rationalized in terms of intermolecular interactions. Hydrogen bonding of the hydroxyl group to one ring nitrogen atom takes place along with a nitro group π interaction yielding two-dimensional ribbons similar to the structure of **1**. However, in

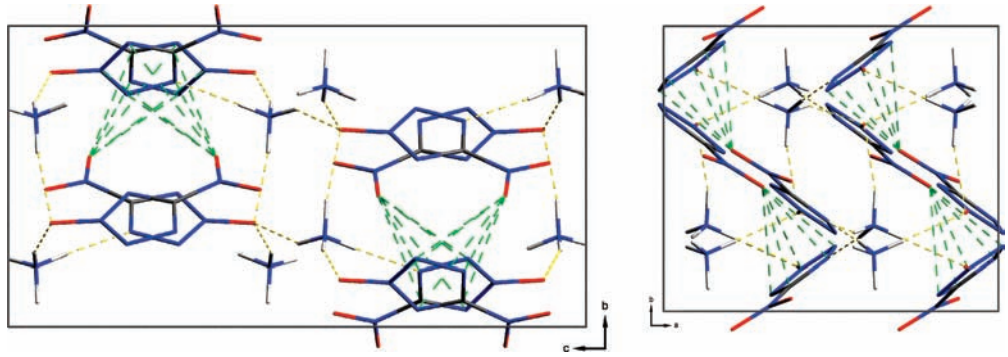

Figure 3. Unit cell packing of **1** (ANTX, ammonium 5-nitrotetrazolate-2*N*-oxide), viewed along the *a* axis (left) and *c* axis (right). Yellow dashed lines indicate intermolecular hydrogen bonding (N6−H6A···O1[i], N6−H6A···N2[i], N6−H6B···N4[ii], N6−H6C···O1[iii], N6−H6D···O1). The green dashed lines indicate the interaction between the O3-oxygen atom of the nitro group and the π electrons of the tetrazole ring (contact distance: 3.4022(10) Å [O3···Cg(π_{Ring})[iv]]; Symmetry code: (i) $^1/_2 - x$, $^1/_2 + y$, z; (ii) $-^1/_2 + x$, y, $^1/_2 - z$; (iii) $-^1/_2 + x$, $^1/_2 - y$, $-z$; (iv) $-^1/_2 + x$, y, $^1/_2 - z$.

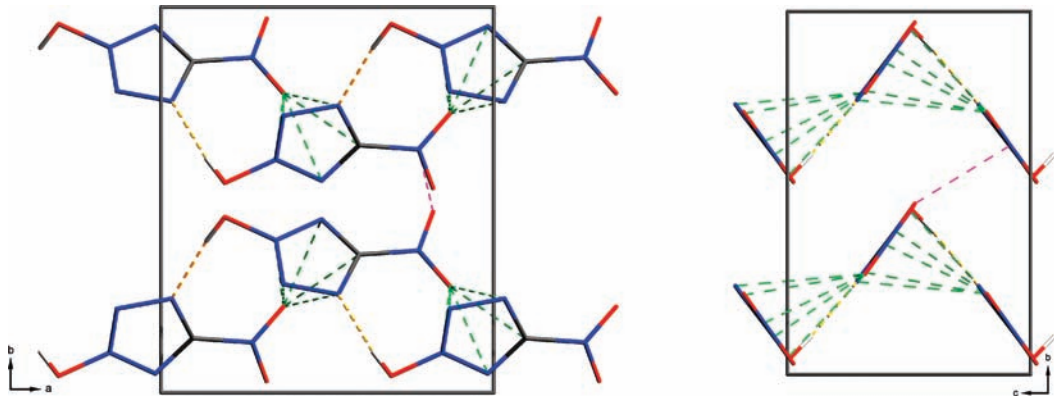

Figure 5. Unit cell packing of **2** (5-nitro-2-hydroxy-tetrazole, HNTX), viewed along the *c* axis (left) and *a* axis (right). Yellow dashed lines indicate intermolecular hydrogen bonding (O1−H1···N4^{i}). The pink dashed line represents a dipolar nitro group interactions between two neighboring N5/O2/O3 nitro groups (contact distance: 2.8200(17) Å [N5···O3^{ii}]; 2.966(4) Å [O6···O15^{iv}]). The green dashed lines indicate the interaction between the O2-oxygen atom of the nitro group and the π electrons of the tetrazole ring (contact distance: 2.8897(13) Å [O2···Cg(π_{Ring})]; Symmetry code: (i) $-^1/_2 + x$, $^1/_2 - y$, $-^1/_2 + z$; (ii) x, $-y$, $-^1/_2 + z$; (iii) $^1/_2 + x$, $^1/_2 - y$, $^1/_2 + z$.

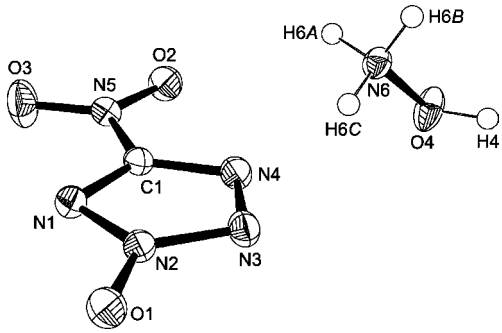

Figure 6. ORTEP representation of the molecular structure of **3** (HxNTX, hydroxylammonium 5-nitrotetrazolate-2*N*-oxide) in the crystalline state. Displacement ellipsoids are shown at the 50% probability level.

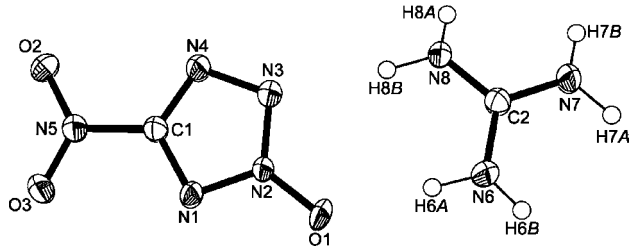

Figure 7. ORTEP representation of the molecular structure of **4** (GNTX, guanidinium 5-nitrotetrazolate-2*N*-oxide) in the crystalline state. Displacement ellipsoids are shown at the 50% probability level.

the case of the free acid, these ribbons are interconnected through a dipolar nitro group interaction (Figure 5).

The structure of **3** (HxNTX, hydroxylammonium 5-nitrotetrazolate-2*N*-oxide) at 173 K has monoclinic ($P2_1/c$) symmetry. The asymmetric unit consists of one molecule (Figure 6). **3** displays a high density of 1.850(2) g cm^{-3}.

The structure of **4** (GNTX, guanidinium 5-nitrotetrazolate-2*N*-oxide) at 173 K has triclinic ($P\bar{1}$) symmetry. The asymmetric unit consists of one molecule (Figure 7).

The structure of **5** (AGNTX, aminoguanidinium 5-nitrotetrazolate-2*N*-oxide) at 173 K has monoclinic ($P2_1/c$) symmetry. The asymmetric unit consists of one molecule (Figure 8).

The structure of **6** (DAGNTX, diaminoguanidinium 5-nitrotetrazolate-2*N*-oxide) at 173 K has triclinic ($P\bar{1}$) symmetry. The asymmetric unit consists of one molecule (Figure 9). The nitrotetrazolate-2*N*-oxide anion is disordered such that 31% of anions are rotated 180° around the center of gravity. In Figure 9 only one orientation is shown.

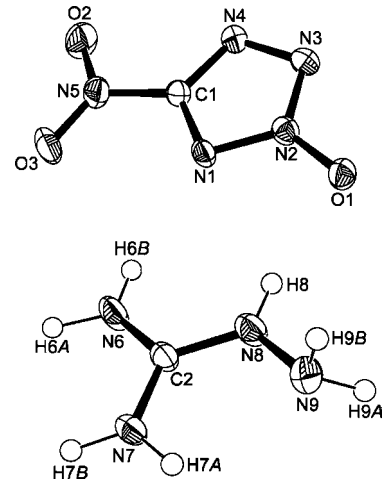

Figure 8. ORTEP representation of the molecular structure of **5** (AGNTX, aminoguanidinium 5-nitrotetrazolate-2*N*-oxide) in the crystalline state. Displacement ellipsoids are shown at the 50% probability level.

The structure of **8** (TAGNTX, triaminoguanidinium 5-nitrotetrazolate-2*N*-oxide) at 173 K has monoclinic ($P2_1/c$) symmetry. The asymmetric unit consists of one molecule (Figure 10).

Physicochemical Properties. Since all the materials studied are energetic compounds, their energetic behaviors were investigated.

Thermal Behavior. The thermal behaviors of all the nitrogen-rich salts prepared were investigated on a Linseis PT10 DSC with heating rates of 5 °C min^{-1} using ∼1.5 mg of material. Many of the compounds decompose violently, especially ANTX and HxNTX which rupture the DSC pans. The triaminoguanidinium salt shows the lowest decomposition temperature of 153 °C, and the highest decomposition temperature is shown by the guanidinium salt with at 211 °C. Large liquid ranges are seen for DAGNTX and TAGNTX making them potential melt-cast explosives. Table 4 contains the decomposition temperatures and melting points for nitrogen-rich materials **1**, **3**−**5**, and **7**−**8**. The substituted guanidinium salts show decreased thermal stability with an increased number of amino substituents on the guanidinium cation. To compare the decomposition temperatures with the nitrogen-rich nitrotetrazolates DSC experiments were also carried out with a heating rate of 10 °C min^{-1} as was used for the nitrotetrazolates in the literature[21] (Table 4). The use of

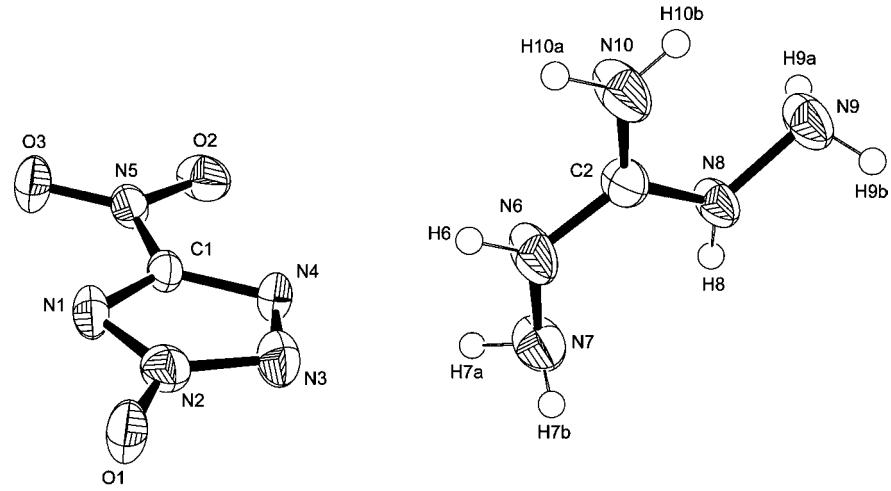

Figure 9. ORTEP representation of the molecular structure of **6** (DAGNTX, 1,3-diaminoguanidinium 5-nitrotetrazolate-2*N*-oxide) in the crystalline state. Displacement ellipsoids are shown at the 50% probability level.

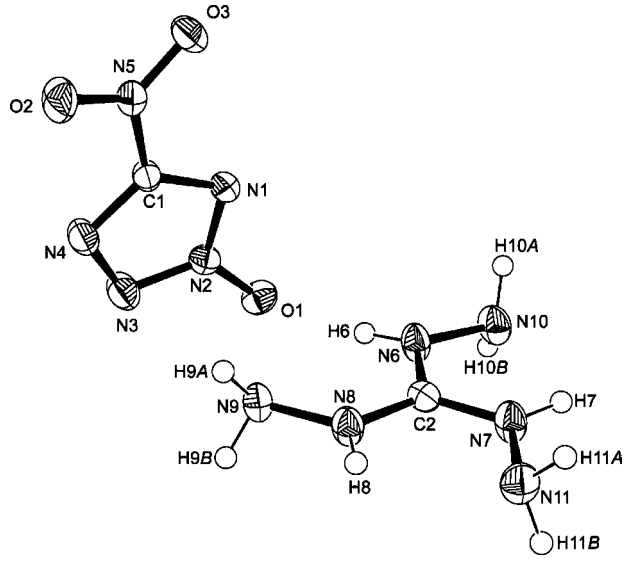

Figure 10. ORTEP representation of the molecular structure of **8** (TAGNTX, triaminoguanidinium 5-nitrotetrazolate-2*N*-oxide) in the crystalline state. Displacement ellipsoids are shown at the 50% probability level.

Table 4. Thermal Behavior of Nitrogen-Rich Salts

Compound	Abbreviation	T_m (°C) (5 °C min^{-1})	T_{dec} (°C) (5 °C min^{-1})	T_{dec} (°C) (10 °C min^{-1})
1	ANTX	165	173	179
3	HxNTX	149	157	164
4	GNTX	198	211	219
5	AGNTX	167	185	196
7	DAGNTX	83	174	184
8	TAGNTX	82	153	162

a faster heating rate is known to give higher decomposition temperatures.[48] When the decomposition temperatures are compared to those possessed by the nitrogen-rich nitrotetrazolates[21] the nitrogen-rich nitrotetrazolate-2*N*-oxides generally decompose at a lower temperature with the exception of **4** which is comparable. The high decomposition temperature for the guanidinium salt (**4**) indicates the nitrotetrazole-2*N*-oxide anion is capable of forming highly thermally stable salts with the appropriate cation pairing; unfortunately, many of the cations we paired with the nitrotetrazolate-2*N*-oxide anion proved to have lower thermal stability.

Heats of Formation. For a complete discussion on the methods used please see the Supporting Information. When compared to the corresponding heats of formation of the nitrogen-rich nitrotetrazolates[17] all the nitrotetrazolate-2*N*-oxides possess lower heats of formation. For example, the ammonium salt shows a decrease from 191.4 to 152.0 kJ mol^{-1} and the triaminoguanidinium salt shows a decrease from 601.8 to 471.5 kJ mol^{-1} between nitrotetrazolate and nitrotetrazolate-2*N*-oxide. However, the acid (**2**) has an increased heat of formation of 308.6 kJ mol^{-1} in contrast to the lower heat of formation of 281.0 kJ mol^{-1} in free nitrotetrazole[35] as a consequence of the proton lying on oxygen as opposed to a nitrogen atom. For a summary of the heat of formation results please see Table 5.

Detonation Parameters. Calculations of the detonation parameters (Table 5) were performed with the program package EXPLO5 using the version 5.03[49] as well as version 5.04[50] (values in brackets), in which several parameters have been modified. The input was made using the sum formula, energy of formation, and the experimentally determined densities (X-ray). The program is based on the chemical equilibrium, steady-state model of detonation. It uses the Becker−Kistiakowsky−Wilson's equation of state (BKW EOS) for gaseous detonation products and Cowan−Fickett's equation of state for solid carbon.[51−54] The calculation of the equilibrium composition of the detonation products is done by applying modified White, Johnson, and Dantzig's free energy minimization technique. The program is designed to enable the calculation of detonation parameters at the CJ point. The BKW equation in the following form was used with the BKWN set of parameters (α, β, κ, θ) as stated below the equations, X_i being the molar fraction of *i*-th gaseous product, and k_i being the molar covolume of the *i*-th gaseous product:

(48) Pinheiro, G. F.; Lourenco, V. L.; Iha, K. *J. Therm. Anal. Calorim.* **2002**, *67*, 445–452.

(49) Sućeska, M. *EXPLO5.3 program*; Zagreb, Croatia, 2009.
(50) Sućeska, M. *EXPLO5.4 program*; Zagreb, Croatia, 2010.
(51) Sućeska, M. *Mater. Sci. Forum* **2004**, *465−466*, 325–330.
(52) Sućeska, M. *Propellants, Explos., Pyrotech.* **1991**, *16*, 197–202.
(53) Sućeska, M. *Propellants, Explos., Pyrotech.* **1999**, *24*, 280–285.
(54) Hobbs, M. L.; Baer, M. R. *Proceedings of the 10th Symposium (International) on Detonation*, ONR 33395-12, Boston, MA, July 12−16, 1993, p 409.

Table 5. Energetic Properties and Detonation Parameters

	1	**2**	**3**	**4**	**5**	**7**	**8**	RDX
Formula	$CH_4N_6O_3$	CHN_5O_3	$CH_4N_6O_4$	$C_2H_6N_8O_3$	$C_2H_7N_9O_3$	$C_2H_8N_{10}O_3$	$C_2H_9N_{11}O_3$	$C_3H_6N_6O_6$
FW (g mol^{-1})	148.11	131.07	164.11	190.16	205.18	220.20	235.16	222.12
IS^a (J)	7	N.D.	4	>40	20	40	25	7.5
FS^b (N)	120	N.D.	60	252	112	120	72	120
ESD^c (J)	0.25	N.D.	0.05	0.20	0.20	0.20	0.20	0.1−0.2
N^d (%)	56.75	52.23	51.22	58.94	61.45	63.62	65.52	37.84
Ω^e (%)	−10.80	6.10	0.00	−33.66	−35.09	−36.33	−37.42	−21.61
$T_{Dec}{}^f$ (°C)	173	∼120	157	211	185	174	153	210
ρ^g (g cm^{-3})	1.730	1.940	1.85	1.698	1.697	1.687	1.639	1.80
$\Delta_f H_m{}^{\circ h}$/ kJ mol^{-1}	152.0	308.6	218.7	136.7	256.4	361.0	471.5	70
$\Delta_f U^{\circ i}$/ kJ kg^{-1}	1135.0	2439.3	1438.5	829.6	1364.3	1757.5	2125.6	417
				Calculated Values by EXPLO5^o				
$\Delta_{Ex}U^{\circ j}$/ kJ kg^{-1}	5509 (5627)	6124 (6221)	6535 (6521)	4570 (4580)	4886 (4927)	5158 (5145)	5376 (5355)	6038 (6125)
$T_{det}{}^k$ (K)	4218 (4094)	5092 (4949)	4763 (4596)	3500 (3380)	3601 (3491)	3654 (3542)	3749 (3604)	4368 (4236)
$P_{CJ}{}^l$ (GPa)	32.2 (32.8)	40.4 (41.6)	39.0 (41.0)	26.6 (27.4)	28.5 (29.0)	29.2 (29.9)	29.4 (29.2)	34.1 (34.9)
$V_{Det}{}^m$ (m s^{-1})	8885 (8767)	9447 (9283)	9499 (9381)	8201 (8270)	8514 (8503)	8686 (8639)	8768 (8617)	8906 (8748)
$V_o{}^n$ (L kg^{-1})	858 (828)	730 (725)	827 (816)	830 (821)	847 (836)	863 (848)	878 (858)	793 (739)

[a] BAM drophammer. [b] BAM impact. [c] Electrical spark sensitivity. [d] Nitrogen content. [e] Oxygen balance. [f] Decomposition temperature from DSC (5 °C min^{-1}). [g] Density from X-ray diffraction. [h] Calculated molar enthalpy of formation. [i] Energy of formation. [j] Total energy of detonation. [k] Explosion temperature. [l] Detonation Pressure. [m] Detonation velocity. [n] Volume of detonation products. [o] Explo5.03 (Explo5.04).

$$pV/RT = 1 + xe^{\beta x} \quad x = (\kappa \sum X_i k_i)/[V(T + \theta)]^{\alpha}$$

$$\alpha = 0.5,\ \beta = 0.176,\ \kappa = 14.71,\ \theta = 6620 \qquad \text{(EXPLO 5.03)}$$

$$\alpha = 0.5,\ \beta = 0.96,\ \kappa = 17.56,\ \theta = 4950 \qquad \text{(EXPLO 5.04)}$$

The detonation parameters calculated with the EXPLO5 program are summarized in Table 5.

The ammonium (**1**), diaminoguanidinium (**7**), and triaminoguanidinium (**8**) salts of nitrotetrazolate-2*N*-oxide show detonation properties (detonation velocity and pressure) similar to those of RDX making both of these compounds potential green replacements for RDX. The thermal stabilities of the ammonium and diaminoguanidinium salts are acceptable for this use; however triaminoguanidinium may prove to be insufficient. The acid (**2**) and hydroxylammonium salt (**3**) have detonation characteristics outperforming HMX, one of the most powerful secondary explosives in use; however, their thermal stabilities and the extremely deliquescent nature of the free acid will likely preclude application. When the nitrogen-rich nitrotetrazolate-2*N*-oxides are compared to the corresponding nitrotetrazolates[21] a marked performance increase is seen. When detonation velocities are compared, the magnitude of the increase ranges from almost 1000 ms^{-1} for the ammonium salt to only 300 ms^{-1} for the triaminoguanidinium salt. The lower gains in energetic performance for the substituted guanidines are a result of the lower improvement of density when compared with the ammonium salts.

Sensitivities. For initial safety testing, the impact, friction, and electrostatic discharge sensitivity tests of the prepared nitrogen-rich salts were carried out.[55,56] The impact sensitivity tests were carried out according to STANAG 4489[57] and were modified according to instruction[58] using a BAM (Bundesanstalt für Materialforschung[56]) drophammer.[59] The friction sensitivity tests were carried out according to STANAG 2287[60] and were modified according to instruction[61] using a BAM friction tester. Due to the extremely deliquescent nature of the acid **2** sensitivy tests were unable to be carried out with any semblance of accuracy as water is extremely efficient at reducing the sensitivity of energetic materials. The sensitivities of the salts range from sensitive to insensitive according to the UN Recommendations on the Transport of Dangerous Goods.[62] Electrostatic sensitivity tests were performed on all materials using a small scale electric spark tester ESD 2010EN (OZM Research[63]) operating with a "Winspark 1.15" Software package.[64] At the sensitive side of the scale are the ammonium (**1**) and hydroxylammonium (**3**) salts with impact sensitivities of 4 and 7 J, respectively. This is slightly lower than and comparable to RDX, respectively. In contrast the (substituted) guanidinium salts (**4**−**8**) have sensitivities much safer than that of RDX

(55) Sućeska, M. *Test Methods for Explosives*; Springer: New York, 1995; p 21 (impact), p 27 (friction).
(56) www.bam.de.
(57) NATO standardization agreement (STANAG) on explosives, *impact sensitivity tests*, no. 4489, Ed. 1, Sept. 17, 1999.
(58) WIWEB-Standardarbeitsanweisung 4-5.1.02, Ermittlung der Explosionsgefährlichkeit, hier der Schlagempfindlichkeit mit dem Fallhammer, Nov. 8, 2002.
(59) http://www.reichel-partner.de.
(60) NATO standardization agreement (STANAG) on explosives, *friction sensitivity tests*, no. 4487, Ed. 1, Aug. 22, 2002.
(61) WIWEB-Standardarbeitsanweisung 4-5.1.03, Ermittlung der Explosionsgefährlichkeit oder der Reibeempfindlichkeit mit dem Reibeapparat, Nov. 8, 2002.
(62) Impact: Insensitive > 40 J, less sensitive ≥ 35 J, sensitive ≥ 4 J, very sensitive ≤ 3 J; Friction Insensitive > 360 N, less sensitive = 360 N, sensitive < 360 N and > 80 N, very sensitive ≤ 80 N, extremely sensitive ≤ 10 N. According to the UN Recommendations on the Transport of Dangerous Goods.
(63) Skinner, D.; Olson, D.; Block-Bolten, A. *Propellants, Explos., Pyrotech.* **1998**, *23*, 34–42.
(64) http://www.ozm.cz/testinginstruments/small-scale-electrostatic-discharge-tester.htm.

ranging from 20 to greater than 40 J. Such sensitivities are desired for the safe explosives used in insensitive munitions (IMs). In all cases with the exception of the aminoguanidinium salt (**5**) all salts of nitrotetrazolate-2*N*-oxide are less sensitive than the corresponding nitrotetrazolate salt.[17]

Conclusions

It is possible to oxidize the nitrotetrazolate anion to the nitrotetrazolate-2*N*-oxide anion under mild, aqueous conditions in high yield. Upon protonation, the nitrotetrazolate-2*N*-oxide anion forms 2-hydroxy-5-nitrotetrazole. Nitrogen-rich nitrotetrazolate-2*N*-oxide salts can be formed via metathesis reactions starting from the now-easily available ammonium nitrotetrazolate-2*N*-oxide, and the molecular and crystal structures of these materials were determined for the first time. Multinuclear NMR, IR, and Raman spectroscopy proved to be valuable tools in characterizing these salts. Computational calculations show energetic, nitrogen-rich nitrotetrazolate-2*N*-oxides to have lower heats of formation than their nitrotetrazolate counterparts.

The nitrotetrazolate-2*N*-oxides exibit higher densities than nitrotetrazolates due to the greater numbers of intermolecular interactions allowed by the *N*-oxides. Due to high experimentally determined densities, nitrogen-rich nitrotetrazolate-2*N*-oxides are high-performance energetic materials. Decomposition temperatures range from 153 to 211 °C indicating the nitrotetrazolate-2*N*-oxide anion has the ability to form thermally stable energetic materials with appropriate cation pairing, despite being slightly less thermally stable then the corresponding nitrotetrazolates. The experimentally determined sensitivities of the nitrotetrazolate-2*N*-oxides are in general lower than those for the nitrotetrazolates, ranging from sensitivities comparable to that of RDX to insensitive.

Experimental Section

All reagents and solvents were used as received (Sigma-Aldrich, Fluka, Acros Organics) if not stated otherwise. Ammonium nitrotetrazolate hemihydrate was prepared according to the literature procedure.[21] Melting and decomposition points were measured with a Linseis PT10 DSC using heating rates of 5 °C min^{-1}, which were checked with a Büchi Melting Point B-450 apparatus. ^{1}H, ^{13}C, and ^{15}N NMR spectra were measured with a JEOL instrument. All chemical shifts are quoted in ppm relative to TMS (^{1}H, ^{13}C) or nitromethane (^{15}N). Infrared spectra were measured with a Perkin-Elmer Spektrum One FT-IR instrument. Raman spectra were measured with a Perkin-Elmer Spektrum 2000R NIR FT-Raman instrument equipped with a Nd:YAG laser (1064 nm). Elemental analyses were performed with a Netsch STA 429 simultaneous thermal analyzer. Sensitivity data were determined using a BAM drophammer and a BAM friction tester. The electrostatic sensitivity tests were carried out using an Electric Spark Tester ESD 2010 EN (OZM Research) operating with the "Winspark 1.15" software package.

CAUTION! *5-Nitrotetrazole-2N-oxide (**2**) and its salts (**1**, **3**−**8**) are all energetic compounds with sensitivity to various stimuli. While we encountered no issues in the handling of these materials, proper protective measures (face shield, ear protection, body armor, Kevlar gloves, and earthened equipment) should be used at all times.*

Ammonium 5-Nitrotetrazolate-2*N*-oxide (ANTX, 1). Ammonium nitrotetrazolate hemihydrate (1.5 g, 11 mmol) was dissolved in 25 mL of distilled water. The solution was heated to 40 °C, and 21.0 g (34 mmol) of oxone were added in small portions over 1 h. The suspension was stirred at 40 °C for three days followed by the addition of sufficient water to dissolve all solids. The solution was chilled, and 10 mL of concentrated sulfuric acid were added dropwise. The yellow solution was extracted with 30 mL portions of ether 5 times or until the aqueous layer was colorless. The ether extracts were combined and dried over anhydrous magnesium sulfate followed by evaporation of the ether under vacuum to an oil. The oil was dissolved in 10 mL of distilled water producing a yellow solution, which was chilled, and 5.5 mL of ammonia were added dropwise keeping the solution cold. The solution was evaporated under vacuum, and the yellow solid obtained was recrystallized from acetonitrile yielding 1.20 g (88%) of ammonim nitrotetrazolate-2*N*-oxide. Mp: 165 °C, 173 °C (dec); IR (cm^{-1}) $\tilde{\nu}$ = 3154 (m), 3022 (m), 2867 (m), 2684(w), 2508 (w), 2325 (w), 2269 (w), 2142 (w), 2084 (w), 1846 (w), 1776 (w), 1698 (w), 1678 (w), 1625 (w), 1538 (s), 1470 (m), 1459 (m), 1428 (s), 1411 (s), 1373 (s), 1316 (s), 1270 (s), 1251 (m), 1235 (s), 1192 (m), 1143 (w), 1092 (m), 1061 (m), 1003 (m), 846 (m), 773 (m), 699(w), 660 (m); Raman (1064 nm): $\tilde{\nu}$ = 2516 (2), 2325 (2), 1560 (3), 1544 (1), 1497 (1), 1442 (5), 1414 (100), 1380 (2), 1315 (19), 1274 (3), 1237 (3), 1099 (85), 1064 (10), 1005 (97), 850 (2), 766 (4), 608 (4), 485 (5), 431 (2), 227 (6); ^{1}H NMR (DMSO-d_6) δ (ppm) = 7.30 (s, 4H, NH_4); ^{13}C NMR (DMSO-d_6) δ (ppm) = 158.4 (s, 1C, CN_5O_3). ^{15}N NMR (DMSO-d_6) δ (ppm) = −28.8 (s, 1N, N3), −30.1 (s, 1N, N5, NO_2), −33.3 (s, 1N N2, N−O), −75.6 (s, 1N, N4), −103.4 (s, 1N, N1), −360.3 (s, 1N,N6, NH_4); *m*/*z*: (FAB−) 130.1; (CN_5O_3) *m*/*z*: (FAB+) 18.1 (NH_4); EA ($CH_4N_6O_3$, 148.08 g mol^{-1}) calcd: C, 8.11; N, 56.75; H, 2.72%. Found: C, 8.09; N, 56.30; H, 2.68%. BAM impact: 7 J; BAM friction: 120 N; ESD: 250 mJ.

5-Nitrotetrazole-2*N*-oxide = 5-Nitro-2-hydroxytetrazole (2). ANTX (0.50 g, 3.4 mmol) was dissolved in 10 mL of distilled water, and an excess of concentrated sulfuric acid was added (∼5 mL) slowly while the solution chilled in an ice bath. The yellow solution was extracted with 5 × 10 mL portions of ether, and the ether extracts dried over magnesium sulfate. After evaporation of ether under vacuum, 0.38 g of HNTX was obtained (86%). IR (cm^{-1}) $\tilde{\nu}$ = 3422 (w, br), 2666 (m, br), 1710 (w, br), 1574 (s), 1471 (m), 1418 (m), 1360 (m), 1321 (m), 1248 (m), 1140 (s), 1078 (s), 1034 (s), 890 (m), 845 (s), 757 (w), 676 (w); Raman (1064 nm): $\tilde{\nu}$ = 2953 (8), 1580 (15), 1544 (4), 1473 (27), 1422 (100), 1362 (5), 1325 (13), 1252 (15), 1179 (21), 1081 (14), 1036 (83), 849 (11), 773 (8), 761 (19), 586 (5), 571 (2), 549 (3), 461 (7), 412 (11), 369 (3), 327 (3), 237 (8); ^{1}H NMR (THF-d_8) δ (ppm) = 12.99 (s, 1H, O−*H*); ^{13}C NMR (THF-d_8) δ (ppm) = 162.1 (s, 1C, CN_5O_3); ^{15}N NMR (THF-d_8) δ (ppm) = −18.0 (s, 1N, N3), −34.4 (s, 1N, N5, NO_2), −64.1 (s, 1N N2, N−O), −72.6 (s, 1N, N4), −94.2 (s, 1N, N1), −360.3 (s, 1N,N6, NH_4); EA (CN_5O_3H, 99.05 g mol^{-1}) calcd: C, 12.13; N, 70.70; H, 1.02%. Found: not determinable due to high sensitivity. Impact, Friction, and ESD sensitivity: not determinable due to high deliquescency.

Hydroxylammonium 5-Nitrotetrazolate-2*N*-oxide (HxNTX, 3). ANTX (1.0 g, 6.8 mmol) was dissolved in 10 mL of distilled water, and the solution was passed through a column of Amberlyst15 ion-exchange resin loaded with hydroxyammonium cation at a slow rate (∼1 h). The yellow column effluent was evaporated to dryness and recrystallized from acetonitrile yielding 0.84 g (88%) of HxNTX after drying under high vacuum. Mp: 149 °C, 157 (dec); IR (cm^{-1}) $\tilde{\nu}$ = 3224 (m), 3134 (m), 3033 (m), 2931 (m), 2815 (m), 2698 (m), 2522 (w), 1620 (w), 1591 (w), 1551 (s), 1512 (s), 1471 (s), 1459 (m), 1419 (vs), 1383 (m), 1315 (s), 1229 (s), 1164 (s), 1104 (m), 1058 (m), 1009 (s), 849 (s), 775 (s), 696 (w), 658 (m); Raman (1064 nm): $\tilde{\nu}$ = 2528 (2), 1592 (1), 1549 (3), 1473 (12), 1460 (6), 1425 (45), 1318 (100), 1234 (2), 1172 (5), 1112 (84), 1060, (21), 1010 (91), 855 (4), 765 (6), 604 (5), 487 (4), 277 (4); ^{1}H NMR (DMSO-d_6) δ (ppm) = 10.06 (s, br, 4H, NOH_4); ^{13}C NMR (DMSO-d_6) δ (ppm) = 158.0 (s, 1C, CN_5O_3); ^{15}N NMR (DMSO-d_6) δ (ppm) = −27.8 (s, 1N, N3), −29.5 (s 1N N, NO_2), −32.4 (s, 1N, N2, N−O), −74.7 (s, 1N, N4), −102.7 (s, 1N, N1), −298.9 (N6, NH_4O+); *m*/*z*: (FAB−) 130.1 (CN_5O_3); *m*/*z*: (FAB+) 34.0 (NH_4O); EA ($CN_6H_4O_4$, 164.08) calcd: C, 7.32; N, 51.22; H, 2.46%; Found: C, 7.18; N, 50.75; H, 2.18%; BAM impact: 4 J; BAM friction: 60 N; ESD: 50 mJ.

Guanidinium 5-Nitrotetrazolate-2*N*-oxide (GNTX, 4). ANTX (0.500 g, 3.4 mmol) was dissolved in 50 mL of ethanol. Guanidine carbonate (0.305 g, 1.7 mmol) was added, and the solution was refluxed for 18 h. The yellow solution was evaporated under vacuum

to 15 mL and chilled to 0 °C yielding 0.47 g of GNTX after filtration. The filtrate was concentrated to half volume yielding another 0.10 g of GNTX after cooling and filtration for a combined yield of 88%. Mp: 198 °C, 211 °C (dec); IR (cm^{-1}) $\tilde{\nu}$ = 3446(m), 3403 (m), 3359 (m), 3271 (m), 3201 (m), 2851 (w), 2790 (w), 2505 (w), 2177(w), 1661 (s), 1566 (m), 1537 (m), 2472 (s), 1460 (m), 1431(s), 1392(m), 1319(s), 1226 (m), 1082 (m), 1051(m), 1003(m), 844 (m), 786 (s), 739 (w), 703 (w), 688(w); Raman (1064 nm): $\tilde{\nu}$ = 3274 (2), 1648 (1), 1576 (1), 1552 (3), 1474 (2), 1424 (100), 1411 (8), 1317 (11), 1090 (29), 1052 (10), 1011 (8), 1003 (49), 787 (3), 762 (2), 613 (2), 535 (4), 484 (3), 432 (2), 236 (2), 122 (28); ^{1}H NMR (DMSO-d_6) δ (ppm) = 6.87 (s, broad, 6H, N*H*); ^{13}C NMR (DMSO-d_6) δ (ppm) = 158.2 (s, 1C, *C*(NH_2)$_3$), 157.6 (s, 1C, CN_5O_3); ^{15}N NMR (DMSO-d_6) δ (ppm) = −28.7 (s, 1N, N3), −29.9 (s, 1N, N, *N*O_2), −31.5 (s, 1N, N2, *N*−O), −75.4 (s, 1N, N4), −103.8 (s, 1N, N1), −306.5 (s, 3N, N6/N7/N8, *C*(NH_2)$_3$); *m*/*z*: (FAB−) 130.1 (CN_5O_3); *m*/*z*: (FAB+) 60.1 (CN_3H_6); EA ($C_2N_8H_6O_3$, 190.12) calcd: C, 12.63; N, 58.94; H, 3.18%. Found: C, 12.77; N, 58.43; H, 3.14%; BAM impact: > 40 J; BAM friction: 252 N; ESD: 0.20 mJ.

Aminoguanidinium 5-Nitrotetrazolate-2*N*-oxide (AGNTX, 5). ANTX (0.70 g, 4.7 mmol) was dissolved in 20 mL of ethanol, and to this was added 0.64 g (4.7 mmol) of aminoguanidine bicarbonate; the solution was then refluxed for 18 h. The solution had some crystals present after refluxing, and hot ethanol was added until dissolution followed by filtration while hot. The filtrate was allowed to slowly cool to 0 °C yielding after filtration 0.66 g of crystalline AGNTX. Evaporation of the filtrate to half volume under vacuum followed by chilling to 0 °C yielded 0.25 g more of AGNTX for a combined yield of 94%. Mp: 167 °C, 185 °C (dec); IR (cm^{-1}) $\tilde{\nu}$ = 3413 (m), 3360 (m), 3226 (m), 3170 (m), 2851 (w), 2634 (w), 2508 (w), 2163 (w), 1669 (vs), 1648 (s), 1599 (m), 1540 (s), 1473 (s), 1460 (m), 1433 (s), 1395 (m), 1318 (s), 1232 (m), 1198 (m), 1108 (m), 1086 (m), 1054(w), 1008 (m), 971 (w), 935 (s), 843(m), 784 (m), 742 (w), 702 (w), 656 (w); Raman (1064 nm): $\tilde{\nu}$ = 3361 (2), 3267 (2), 1681 (1), 1563 (2), 1541 (3), 1475 (4), 1425 (100), 1320 (11), 1232 (2), 1090 (37), 1055 (15), 1009 (69), 970 (3), 942 (1), 850 (1), 787 (3), 761 (4), 613 (3), 509 (2), 482 (4), 235 (3); ^{1}H NMR (DMSO-d_6) δ (ppm) = 8.53 (s, 1H C−N*H*−N), 7.22 (s, broad, 2H, C−NH_2), 6.76 (s, broad, 2H, C−NH_2), 4.64 (s, 2H, N−NH_2); ^{13}C NMR (DMSO-d_6) δ (ppm) = 159.2 (s, 1C, *C*(NH_2)$_2$($NHNH_2$)), 157.8 (s, 1C, CN_5O_3); ^{15}N NMR (DMSO-d_6) δ (ppm) = −29.3 (s, 1N, N3), −29.9 (s 1N N, *N*O_2), −33.5 (s, 1N, N2, *N*−O), −75.8 (s, 1N, N4), −103.3 (s, 1N, N1), −307.6 (s, 1N C−*N*H−NH_2), −314.1 (s, 2N, C−*N*H_2), −326.3 (s, 1N, C−*N*H−NH_2); *m*/*z*: (FAB−) 130.1 (CN_5O_3); *m*/*z*: (FAB+) 75.1 (CN_4H_7); EA ($C_2N_9H_7O_3$, 205.14) calcd: C, 11.71; N, 61.45; H, 3.44%; Found: C, 11.65; N, 61.45; H, 3.34%. BAM impact: 20 J; BAM friction: 112 N; ESD: 0.25 mJ.

Silver 5-Nitrotetrazolate-2*N*-oxide (AgNTX, 6). ANTX (1.50 g, 10 mmol) was dissolved in 15 mL of distilled water. While stirring, a solution of 1.72 g (10 mmol) of silver nitrate in 10 mL of distilled water was added dropwise. The yellow suspension was stirred for 30 min, filtered, and rinsed with 10 mL of distilled water. After drying in the dark 1.99 g (82%) of AgNTX were obtained. IR (cm^{-1}) $\tilde{\nu}$ = 1560 (m), 1550 (m), 1494 (m), 1464 (w), 1432 (s), 1470 (s), 1405 (s), 1375 (m), 1325 (s), 1314 (s), 1232 (m), 1105 (w), 1064 (w), 1054 (w), 1027 (w), 1016 (w), 848 (w), 834 (w), 794 (m), 783 (m), 775 (s), 752 (w), 694 (w), 690 (w), 654 (w); ^{13}C NMR (DMSO-d_6) δ (ppm) = 157.0 (s, 1C, *C*N_5O_3); ^{15}N NMR (DMSO-d_6) δ (ppm) = −31.0 (s, 1N, N5, *N*O_2), −31.9 (s, 1N, N3), −35.3 (s, 1N N2, *N*−O), −82.7 (s, 1N, N4), −105.7 (s, 1N, N1); *m*/*z*: (FAB−) 130.1 (CN_5O_3); *m*/*z*: (FAB+) 107.9 (Ag). EA ($AgCN_5O_3$, 213.88 g mol^{-1}) calcd: C, 5.05; N, 29.44%; Found: C, 4.97; N, 29.22%; BAM impact: 5 J; BAM friction: 120 N; ESD: 50 mJ.

Diaminoguanidinium 5-Nitrotetrazolate-2*N*-oxide (DAGNTX, 7). AgNTX (1.00 g, 4.2 mmol) was added to a solution of 1.00 g (4.2 mmol) of diaminoguanidinium iodide in 20 mL of distilled water, and 0.1 mL of 2 M nitric acid was added. The solution was stirred for 3 h and was filtered in the dark. The yellow filtrate was evaporated to dryness under reduced pressure and recrystallized from ethanol yielding 0.65 g (70%) of DAGNTX. Mp: 82 °C, 174 °C (dec); IR (cm^{-1}) $\tilde{\nu}$ = 3451 (m) 3352 (m), 3277 (m), 1667 (s), 1578 (w), 1531 (m), 1468 (m), 1457 (m), 1420 (s), 1414 (s), 1409(s), 1310 (s), 1239 (w), 1223 (m), 1178 (m), 1120 (w), 1082 (w), 1059 (w), 1044 (w), 978 (s), 845 (m), 782 (s), 758 (w), 702 (w), 658 (s); Raman (1064 nm): $\tilde{\nu}$ = 3358 (1), 3302 (2) 1685 (2), 1545 (3), 1407 (100), 1314 (13), 1224 (5), 1184 (2), 1060 (13), 1048 (45), 985 (60), 846 (1), 786 (3), 759 (2), 609 (2), 544 (2), 486 (5), 362 (2), 235 (3); ^{1}H NMR (DMSO-d_6) δ (ppm) = 8.54 (s, broad, 2H C−N*H*−NH_2), 7.13 (s, broad, 2H, C−NH_2), 4.57 (s, broad, 4H, N−NH_2); ^{13}C NMR (DMSO-d_6) δ (ppm) = 160.3 (s, 1C, *C*(NH_2)($NHNH_2$)$_2$), 157.8 (s, 1C, CN_5O_3); *m*/*z*: (FAB−) 130.1 (CN_5O_3); *m*/*z*: (FAB+) 90.1 (CN_5H_8); EA ($C_2N_{10}H_8O_3$, 220.15) calcd: C, 10.91; N, 63.62; H, 3.66%; Found: C, 11.15; N, 62.94; H, 3.56%; BAM impact: 40 J; BAM friction: 120 N; ESD: 0.20 mJ.

Triaminoguanidinium 5-Nitrotetrazolate-2*N*-oxide (TAGNTX, 8). AgNTX (0.65 g, 2.7 mmol) was added to a solution of 0.39 g (2.7 mmol) of triaminoguanidinium chloride and 0.1 mL of 2 M nitric acid in 20 mL of distilled water. The solution was stirred for 3 h and was filtered in the dark. The yellow filtrate was evaporated to dryness under reduced pressure and recrystallized from ethanol yielding 0.44 g (70%) of TAGNTX. Mp: 82 °C, 153 °C (dec); IR (cm^{-1}) $\tilde{\nu}$ = 3359 (w), 3346 (w), 3320 (w), 3186 (w), 1671 (m), 1547 (m), 1467 (w), 1458 (w), 1419 (s), 1386 (w), 1340 (w), 1310 (s), 1226 (m), 1141 (m), 1131 (m), 1071 (w), 1048 (w), 993 (s), 958 (m), 911 (m), 849 (m), 778 (m), 661 (w), 604 (w); Raman (1064 nm): $\tilde{\nu}$ = 3359 (1), 3263 (1), 1689 (2), 1547 (5), 1420 (84), 1314 (13), 1229 (5), 1200 (2), 1148 (2), 1073 (67), 1049 (26), 996 (100), 895 (4), 849 (2), 782 (1), 760 (3), 702 (1), 638 (3), 599 (2), 486 (4), 424 (2), 337 (1), 202 (3), 86 (43); ^{1}H NMR (DMSO-d_6) δ (ppm) = 8.56 (s, broad, 3H C−N*H*−NH_2), 4.42 (s, broad, 6H, N−NH_2); ^{13}C NMR (DMSO-d_6) δ (ppm) = 159.0 (s, 1C, *C*($NHNH_2$)$_3$), 157.1 (s, 1C, CN_5O_3); *m*/*z*: (FAB−) 130.1 (CN_5O_3); *m*/*z*: (FAB+) 105.1 (CN_8H_9); EA ($C_2N_{11}H_9O_3$, 235.17) calcd: C, 10.21; N, 65.52; H, 3.86%. Found: C, 10.53; N, 64.76; H, 3.74; BAM impact: 25 J; BAM friction: 72 N; ESD: 0.20 mJ.

Acknowledgment. Financial support of this work by the Ludwig-Maximilian University of Munich (LMU), the U.S. Army Research Laboratory (ARL), the Armament Research, Development and Engineering Center (ARDEC), the Strategic Environmental Research and Development Program (SERDP), and the Office of Naval Research (ONR Global, title: "Synthesis and Characterization of New High Energy Dense Oxidizers (HEDO) - NICOP Effort") under Contract Nos. W911NF-09-2-0018 (ARL), W911NF-09-1-0120 (ARDEC), W011NF-09-1-0056 (ARDEC), and 10 WP-SEED01-002/WP-1765 (SERDP) is gratefully acknowledged. The authors acknowledge collaborations with Dr. Mila Krupka (OZM Research, Czech Republic) in the development of new testing and evaluation methods for energetic materials and with Dr. Muhamed Sucesca (Brodarski Institute, Croatia) in the development of new computational codes to predict the detonation and propulsion parameters of novel explosives. We are indebted to and thank Drs. Betsy M. Rice and Brad Forch (ARL, Aberdeen, Proving Ground, MD) and Mr. Gary Chen (ARDEC, Picatinny Arsenal, NJ) for many helpful and inspired discussions and support of our work. Stefan Huber is also thanked for assistance during sensitivity measurements.

Supporting Information Available: CIF files, selected bond lengths and angles, the methodology and details for heats of formation calculation, and complete ref 41. This material is available free of charge via the Internet at http://pubs.acs.org.

JA106892A